Spontaneous collective coherence in driven dissipative cavity arrays

J. Ruiz-Rivas,[1] E. del Valle,[2,*] C. Gies,[3] P. Gartner,[4] and M. J. Hartmann[5,6]
[1]*Departament d'Òptica, Universitat de València, Dr. Moliner 50, 46100 Burjassot, Spain*
[2]*Física Teórica de la Materia Condensada, Universidad Autónoma de Madrid, 28049 Madrid, Spain*
[3]*Institute for Theoretical Physics, University of Bremen, 28334 Bremen, Germany*
[4]*Institute of Physics and Technology of Materials, P.O. Box MG-7, Bucharest-Magurele, Romania*
[5]*Institute of Photonics and Quantum Sciences, Heriot-Watt University, Edinburgh EH14 4AS, United Kingdom*
[6]*Technische Universität München, Physik Department, James Franck Strasse, 85748 Garching, Germany*
(Received 22 January 2014; published 4 September 2014)

We study an array of dissipative tunnel-coupled cavities, each interacting with an incoherently pumped two-level emitter. For cavities in the lasing regime, we find correlations between the light fields of distant cavities, despite the dissipation and the incoherent nature of the pumping mechanism. These correlations decay faster than any power of the distance for arrays in any dimension but become increasingly long ranged with increasing photon tunneling between adjacent cavities. The interaction-dominated and the tunneling-dominated regimes show markedly different scaling of the correlation length which always remains finite due to the finite photon trapping time. We propose a series of observables to characterize the spontaneous buildup of collective coherence in the system.

DOI: 10.1103/PhysRevA.90.033808 PACS number(s): 42.50.Pq, 42.50.Ct, 64.60.Ht, 67.25.dj

I. INTRODUCTION

Arrays of optical or microwave cavities, each interacting strongly with quantum emitters and mutually coupled via the exchange of photons, have been introduced as prototype setups for the study of quantum many-body physics of light [1–3]. Even though ground or thermal equilibrium states of the corresponding quantum many-body systems are challenging to generate in experiments, much of the initial attention has focused on this regime [4–7]. In any realistic experiment with cavity arrays, however, photons are dissipated due to the imperfect confinement of the light, and emitter excitations have finite lifetimes. It is thus crucial and useful to explore the driven-dissipative regime of these structures, where photon losses are continuously compensated by pumping new photons into the cavities. A special role is here taken by the stationary states where photon pumping and losses balance each other in a *dynamical equilibrium*. This regime has thus received considerable attention in recent years, where coherent and strongly correlated phases have been discovered [8–10], but also analogies to quantum Hall physics [11] and topologically protected quantum states [12] have been discussed.

In previous investigations of coupled cavity arrays in driven-dissipative regimes, the pump mechanism that injects photons into the array has been assumed to be a coherent drive at each cavity [8–12]. Therefore any phase coherence between light fields in distant cavities that was seen in these studies can at least in part be attributed to the fixed phase relation between their coherent input drives. Here, in contrast, we show that such a coherence between distant cavities can build up spontaneously, triggered only by physical processes within the array. In this way we address the question of whether a nonequilibrium superfluid or Bose-Einstein condensate can develop in these structures. To this end, we consider a cavity array that is only driven by an incoherent pump which explicitly avoids any external source for a preferred phase relation between photons in different cavities.

In our model, each cavity strongly interacts with a two-level emitter. Whereas both emitters and cavity photons are subject to dissipation processes, the cavities are excited via the emitters only, which are population inverted by an incoherent pump. For a single cavity our model reduces to the previously considered and realized *one-emitter laser* [13–18]. Generalizations of this single cavity model have also been studied for two [19] and multiple emitters [20–22] or emitters supporting multiexciton states [23].

We focus our analysis on the buildup of first-order coherence between the fields in distant cavities as this quantity is typically considered for investigating long-range order and the emergence of superfluidity, e.g., in optical lattices [24]. In cavity arrays these correlations can be measured by recording the interference pattern of the light fields emitted from the individual cavities. We find that collective correlations indeed build up in our setup when the cavities are in the lasing regime. These correlations decay faster than any power of the distance as the distance between the considered cavities tends to infinity for any dimension of the array. As intuitively expected, the associated correlation length increases with increasing photon tunneling between the cavities. For the interaction-dominated regime this increase is logarithmic, whereas it is a power law in the tunneling-dominated regime. Nonetheless, for any nonvanishing cavity decay rate, the correlation length always remains finite.

Related questions are of high relevance for ultracold atoms [25], ions [26], superconducting circuits [27], or exciton-polariton condensates [7]. For the latter, functional renormalization-group approaches showed that correlations at least decay exponentially in isotropic two-dimensional [28] but can be long range in three-dimensional systems [29].

Finally, we also find that the collective coherence buildup manifests strongly in the local cavity properties such as intensity and spectrum of emission. In particular, lasing and its typical photoluminescence (PL) line shape, the Mollow

*elena.delvalle.reboul@gmail.com

triplet [17,30], can be observed far out of resonance between emitter and cavity as a result of the emergence of collective photonic modes.

Suitable experimental platforms for exploring our findings are superconducting circuit [6,31], photonic crystal [32,33], micropillar [34], or waveguide coupled cavities [35], where strong-coupling regimes and coherent photon transfer between cavities have been demonstrated. See also the reviews [4,6,7].

II. MODEL

We consider an array of cavities, each of which interacts with a two-level emitter, and is connected to adjacent cavities via photon tunneling. Our system, cf. Figs. 1(a) and 1(b), is thus described by a Jaynes-Cummings-Hubbard Hamiltonian ($\hbar = 1$),

$$H = \sum_j H_j^{JC} + \sum_{\langle j,l\rangle} J[a_j^\dagger a_l + a_l^\dagger a_j] \tag{1}$$

with $H_j^{JC} = \omega_a a_j^\dagger a_j + \omega_\sigma \sigma_j^\dagger \sigma_j + g(a_j^\dagger \sigma_j + a_j \sigma_j^\dagger)$, where a_j is the photon annihilation operator and $\sigma_j = |g\rangle_j\langle e|_j$ is the emitter de-excitation operator in cavity j. We assume periodic boundary conditions and a homogeneous array with photon tunneling rate J so that all H_j^{JC} feature the same photon frequency ω_a, emitter transition frequency ω_σ, and light-matter coupling g. We are interested in a driven-dissipative regime, where each emitter is excited by an incoherent pump at a rate P_σ [36], and decays spontaneously at a rate γ_σ. The cavity photons in turn are lost at a rate γ_a from each cavity. The dynamics of our system, including these incoherent processes, follows the master equation,

$$\partial_t \rho = -i[H,\rho] + \sum_j \left[\gamma_a \mathcal{L}_{a_j} + \gamma_\sigma \mathcal{L}_{\sigma_j} + P_\sigma \mathcal{L}_{\sigma_j^\dagger}\right](\rho), \tag{2}$$

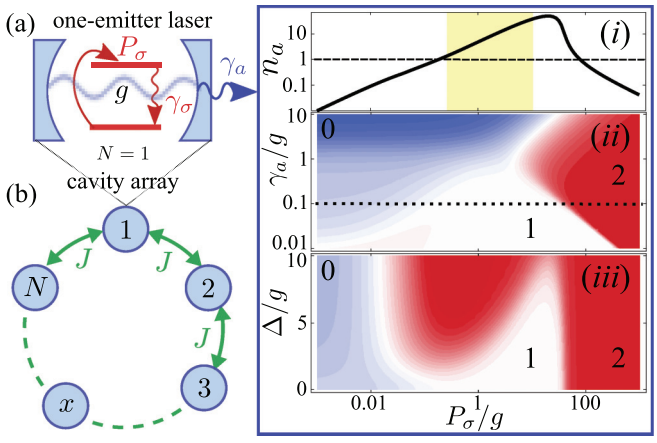

FIG. 1. (Color online) (a) The building block of the array, the one-emitter laser, and its main cavity emission properties: (i) cavity population n_a as a function of P_σ for $\gamma_a = 0.1g$ and $\omega_\sigma = \omega_a$, with the lasing region highlighted in yellow. Below, contour plots of $g^{(2)}$ as a function of P_σ and (ii) γ_a at $\omega_\sigma = \omega_a$, or (iii) $\Delta = \omega_\sigma - \omega_a$ at $\gamma_a = 0.1g$, with $g^{(2)} > 1$ in red, $g^{(2)} = 1$ in white, and $g^{(2)} < 1$ in blue. Also $\gamma_\sigma = 0.01g$ and $J = 0$. (b) Scheme of the total system in one dimension: a circular array of N coupled cavities containing single emitters.

where ρ is the density matrix of the total system and $\mathcal{L}_c(\rho) = \frac{1}{2}(2c\rho c^\dagger - c^\dagger c\rho - \rho c^\dagger c)$. We are interested in the steady state ($\partial_t \rho = 0$) and neglect pure dephasing, since it does not modify the results apart from increasing the decoherence that P_σ already induces. Note that the pumping and decay rates at different sites are completely independent of each other so that our model differs strongly from scenarios where correlations between quantum systems build up via a coupling to a common bath [37].

It is useful to introduce Bloch modes for the photons [9] to diagonalize the cavity part of Hamiltonian (1). For a rectangular lattice of cavities of dimension m and edge length N, these modes read $p_{\vec{k}} = N^{-m/2} \sum_{\vec{r}} e^{i\vec{k}\cdot\vec{r}} a_{\vec{r}}$, where $\vec{r}$ is an m-dimensional lattice site index and the Hamiltonian (1) takes the form

$$H = \sum_{\vec{k}} \omega_{\vec{k}} p_{\vec{k}}^\dagger p_{\vec{k}} + \sum_{\vec{r}} \omega_\sigma \sigma_{\vec{r}}^\dagger \sigma_{\vec{r}} + \sum_{\vec{k},\vec{r}} (G_{\vec{k},\vec{r}} p_{\vec{k}} \sigma_{\vec{r}}^\dagger + \text{H.c.}), \tag{3}$$

with $\omega_{\vec{k}} = \omega_a + 2J\sum_{\alpha=1}^m \cos k_\alpha$, $G_{\vec{k},\vec{r}} = gN^{-m/2} e^{-i\vec{k}\cdot\vec{r}}$, and $k_\alpha = \frac{2\pi}{N}[-N/2 + l_\alpha]$ for N even or $k_\alpha = \frac{2\pi}{N}[-(N+1)/2 + l_\alpha]$ for N odd ($l_\alpha = 1,\ldots,N$). The Bloch modes form a band with their frequencies $\omega_{\vec{k}}$ distributed across the interval $[\omega_a - 2mJ, \omega_a + 2mJ]$. As easily seen, all modes $p_{\vec{k}}$ decay at the same rate γ_a. Hence, we have mapped our model to a set of independent harmonic modes that all couple to the same set of emitters with complex coupling constants $G_{\vec{k},\vec{r}}$. It is useful to define for each mode, the detuning $\Delta_{\vec{k}} = \omega_\sigma - \omega_{\vec{k}}$, the total decoherence rate $\Gamma = \gamma_a + P_\sigma + \gamma_\sigma$, the effective coupling $g_{\vec{k}}^{\text{eff}} = g/\sqrt{1 + (2\Delta_{\vec{k}}/\Gamma)^2}$, and the population transfer from the emitters to the mode (*Purcell rate*) $F_{\vec{k}} = 4(g_{\vec{k}}^{\text{eff}})^2/\Gamma$. Each Bloch mode can thus be driven by coherent excitation exchange with the N emitters.

Before analyzing the entire array we briefly review the properties of a single site, the one-emitter laser, which provides a guideline for our approach. In Fig. 1(a) we show the population, $n_a = \langle a^\dagger a\rangle$, and second-order coherence function of a single cavity, $g^{(2)} = \langle a^\dagger a^\dagger a a\rangle/\langle a^\dagger a\rangle$ as a function of P_σ. In the strong-coupling regime (γ_a, $\gamma_\sigma \ll g$) where we carry out our investigations, one distinguishes [17]: the linear and quantum regimes at low pump ($g^{(2)} < 1$) [20,21,38], the lasing regime ($g^{(2)} = 1$), and the self-quenching and thermal regimes at high pump ($1 < g^{(2)} \leqslant 2$). In this work, we focus on the lasing regime, where the emitter population is half inverted, $n_\sigma = \langle \sigma^\dagger \sigma\rangle \approx n_\sigma^{\text{L}} = 1/2$, and the cavity accumulates a large number of photons, $n_a \approx n_a^{\text{L}} = P_\sigma/2\gamma_a$ [39]. Due to the stochastic nature of the pump, $\langle a\rangle = 0$ [40], and it is through the driving of the photon-assisted polarizations $\langle a^\dagger \sigma\rangle$ [41] that the buildup of coherence in the cavity field is induced, for which $\langle a^\dagger a \sigma^\dagger \sigma\rangle \approx n_a n_\sigma$. These properties allow us to obtain simple rate equations for the populations and polarizations that provide accurate results above the quantum regime, i.e., for $P_\sigma > \gamma_a$, γ_σ [17]. The accuracy of this approach has also been confirmed for $N > 1$ emitters in a single cavity [42]. In turn, in the lower pumping regimes, correlations can be expected to be shorter ranged (as shown in the Appendix B).

III. RATE EQUATIONS

From the above master equation, we derive a hierarchy of coupled equations of motion for correlators (see Appendix A for details) starting with $n_\sigma = \langle \sigma_{\vec{r}}^\dagger \sigma_{\vec{r}} \rangle$ and $n_{\vec{k}} = \langle p_{\vec{k}}^\dagger p_{\vec{k}} \rangle$. We apply the cluster-expansion method up to order 2 [41] to truncate the equations. For the lasing and thermal regimes, this approximation can be expected to be very accurate, thanks to the weak and indirect interactions between modes or emitters, and it further allows us to assume $\langle \sigma_{\vec{r}}^\dagger \sigma_{\vec{s}} \rangle \approx n_\sigma \delta_{\vec{r},\vec{s}}$ and $\langle p_{\vec{k}}^\dagger p_{\vec{q}} \sigma_{\vec{r}}^\dagger \sigma_{\vec{r}} \rangle \approx n_{\vec{k}} n_\sigma \delta_{\vec{k},\vec{q}}$ (indexes $\vec{r}$ and $\vec{s}$ label emitters and $\vec{k}$ and $\vec{q}$ label Bloch modes). We have numerically verified the validity of this approximation by including correlations between emitters in distant cavities. For the steady state we find

$$0 = -\gamma_a n_{\vec{k}} + F_{\vec{k}} n_{\vec{k}} (2n_\sigma - 1) + F_{\vec{k}} n_\sigma, \tag{4a}$$

$$0 = P_\sigma - (P_\sigma + \gamma_\sigma + F) n_\sigma - (2n_\sigma - 1)\tilde{F}, \tag{4b}$$

with $F = N^{-m} \sum_{\vec{k}} F_{\vec{k}}$ and $\tilde{F} = N^{-m} \sum_{\vec{k}} F_{\vec{k}} n_{\vec{k}}$. The polarizations are then given by $\langle p_{\vec{k}}^\dagger \sigma_{\vec{r}} \rangle = i G_{\vec{k},\vec{r}} (n_\sigma - n_{\vec{k}} + 2n_{\vec{k}} n_\sigma)/(\Gamma/2 + i\Delta_{\vec{k}})$ and the local cavity populations by $n_a = N^{-m} \sum_{\vec{k}} n_{\vec{k}}$. Equation (4a) can be solved for $n_{\vec{k}}$ to find

$$n_{\vec{k}} = \frac{\kappa_\sigma \Gamma}{4} \frac{n_\sigma}{(\delta/2)^2 + \Delta_{\vec{k}}^2} \tag{5}$$

with $\delta^2 = \kappa_\sigma \Gamma [\Gamma/\kappa_\sigma - (2n_\sigma - 1)]$ and $\kappa_\sigma = 4g^2/\gamma_a$, the Purcell enhanced decay of an emitter through its local cavity [17]. The distribution of Bloch mode populations is thus a Lorentzian in $\Delta_{\vec{k}}$ with width δ.

The central quantities of interest in our investigation are the normalized correlations between cavity fields in distant cavities. Thanks to the translational invariance in the array (which leads to linear momentum conservation), the Bloch mode correlations vanish, $\langle p_{\vec{k}}^\dagger p_{\vec{q}} \rangle = \delta_{\vec{k},\vec{q}} n_{\vec{k}}$, and the cavity correlations are simply the Fourier transform of the Bloch mode populations $n_{\vec{k}}$,

$$\mathcal{C}(\vec{r}) = \frac{\langle a_{\vec{0}}^\dagger a_{\vec{0}+\vec{r}} \rangle}{\langle a_{\vec{0}}^\dagger a_{\vec{0}} \rangle} = \frac{1}{n_a N^m} \sum_{\vec{k}} e^{-i\vec{k}\cdot\vec{r}} n_{\vec{k}}\,. \tag{6}$$

IV. ASYMPTOTICS OF CORRELATIONS

Inserting Eq. (5) into Eq. (6), we find as a central result that the correlations $\mathcal{C}(\vec{r})$ decay faster than r^{-n} as $r \to \infty$, where $r = |\vec{r}|$, for any positive integer n and lattice dimension m, provided $\delta \neq 0$. The proof of this statement proceeds by showing, via multiple applications of the divergence theorem, that for any power n, $r^n \mathcal{C}(\vec{r}) \to 0$ as $r \to \infty$ (see Sec. IV A). The only possibility for the system to become critical, in the sense that the correlation length of $|\mathcal{C}(\vec{r})|$ diverges, would be that δ vanishes, i.e., that $\Gamma/\kappa_\sigma = (2n_\sigma - 1)$. It is however easily seen that the last term in Eq. (4b) diverges for $N \to \infty$ unless $(2n_\sigma - 1) \to 0$, which, for $\delta = 0$, would imply $\gamma_a = 0$. We, therefore, conclude that any nonvanishing photon decay rate keeps the correlation length finite and thus prevents criticality. On the other hand, in the lasing regime, the higher the cavity quality the longer the correlation length, because a small δ narrows the distribution of the n_k around the resonant mode, corresponding to long correlations in real space (as illustrated in Sec. IV B). These findings are in stark contrast to closed equilibrium systems where, according to the Mermin-Wagner-Hohenberg theorem [43,44], arbitrarily long correlation lengths are ruled out for $m = 1,2$ at nonzero temperatures.

A. Proof of fast decay of correlations

For proving the above statement, we consider the thermodynamic limit of a rectangular m-dimensional lattice of cavities, i.e., where infinitely many cavities are arranged in each lattice direction. We thus have a continuum of momentum modes and $\frac{1}{N^m} \sum_{\vec{k}}$ turns into an integral over the Brillouin zone (BZ) V_k formed by the m-dimensional cube extending from $-\pi$ to π in each direction. The field correlations are then given by

$$\mathcal{C}(\vec{r}) = \frac{1}{n_a (2\pi)^m} \int_{V_k} d^m k e^{-i\vec{k}\cdot\vec{r}} n(\vec{k}), \tag{7}$$

with $\vec{r}$ running on the lattice of m-dimensional vectors with integer coordinates.

For $\delta^2 > 0$, $n(\vec{k})$ is a continuous function of k defined on a finite domain, and therefore it is integrable over V_k. In this case the Riemann-Lebesgue lemma [45] ensures that $\mathcal{C}(\vec{r})$ decays to zero for $\vec{r} \to \infty$. The result we want to show is that this decay is actually faster than any power of r. The proof relies essentially on the fact that $n(\vec{k})$ depends on $\vec{k}$ through cosine functions of the components of $\vec{k}$. As such, $n(\vec{k})$ and all its derivatives are continuous and periodic functions of $\vec{k}$. By periodicity here we mean invariant with respect to translations by reciprocal-lattice vectors, i.e., $n(\vec{k}) = n(\vec{k} + \vec{K})$, where the coordinates of $\vec{K}$ are integer multiples of 2π. In particular, on the surface of the BZ one finds pairwise opposite points, differing by a reciprocal-lattice vector. It follows that in such points $n(\vec{k})$ has equal values, and the same is true for all its derivatives.

For the proof we denote by $\alpha = \{\alpha_1, \alpha_2, \ldots, \alpha_m\}$ a multi-index of natural numbers and by $|\alpha|$ the sum of its components $\alpha_1 + \cdots \alpha_m$. We denote also by r^α the quantity $r_1^{\alpha_1} r_2^{\alpha_2} \cdots r_m^{\alpha_m}$. The result we want to show is that for any α one has $r^\alpha \mathcal{C}(\vec{r}) \to 0$ when $r \to \infty$.

Indeed, multiplying the integral in Eq. (7) with r^α amounts to applying the derivative operator $(i\partial)^\alpha = i^{|\alpha|} \partial_1^{\alpha_1} \cdots \partial_m^{\alpha_m}$ to the plane-wave factor $e^{-i\vec{k}\cdot\vec{r}}$ under the integral. By ∂_i we mean the derivative with respect to k_i. All these derivatives can be transferred upon $n(\vec{k})$ by repeatedly applying the divergence theorem. At each such step, BZ surface integrals are generated. But each of these integrals vanishes, because it involves pairwise equal values of the integrand at the opposite points of the BZ surface. The outer normals to the surface in such points have opposite orientation and this ensures the cancellation. Note that in this argument both the periodicity of the derivatives of $n(\vec{k})$ and that of $e^{-i\vec{k}\cdot\vec{r}}$ are required. The latter is ensured by $\vec{r}$ having integer coordinates.

After transferring all the derivatives one is left with

$$r^\alpha \mathcal{C}(\vec{r}) = \frac{(-i)^{|\alpha|}}{n_a (2\pi)^m} \int_{V_k} d^m k e^{-i\vec{k}\cdot\vec{r}} \partial^\alpha n(\vec{k}). \tag{8}$$

Since the integrand is again a continuous function, the Riemann-Lebesgue lemma can be invoked again, ensuring

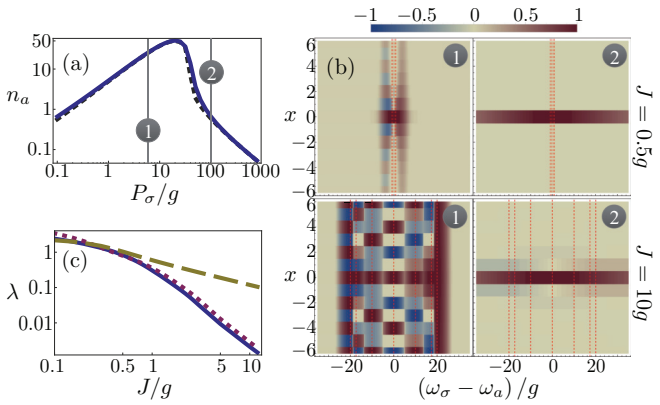

FIG. 2. (Color online) (a) Cavity population n_a for $\omega_\sigma = \omega_a$ as a function of pump P_σ for $J = 0.5g$ (solid blue) and $J = 10g$ (dashed black), with $N = 12$, $\gamma_a = 0.1g$, $\gamma_\sigma = 0.01g$. (b) Corresponding first-order correlations $\mathcal{C}(x)$ as a function of distance x and emitter frequency ω_σ at pump rates (1) and (2) in plot (a). Bloch mode resonances are plotted as vertical dashed red lines. (c) Inverse correlation lengths λ as obtained from fits (see main text) for $N = 108$, $P_\sigma = 5g$, and $\Delta = 0$ (solid), $\Delta = J$ (dotted), or $\Delta = 2J$ (dashed).

that, indeed, $r^\alpha \mathcal{C}(\vec{r})$ goes to zero for large values of the argument. This concludes the proof.

The only possibility that the correlation length could diverge is thus a case where $(2n_\sigma - 1) = \Gamma/\kappa_\sigma$, for which $n_{\vec{k}} \propto \Delta_{\vec{k}}^{-2}$. For this case, however, the last term in Eq. (4b), which reads $(2n_\sigma - 1)\frac{1}{n_a (2\pi)^m}\int_{V_k} d^m k F_{\vec{k}} n_{\vec{k}}$, diverges as long as $(2n_\sigma - 1) \neq 0$. The origin of this divergence is that $\Delta_{\vec{k}}^{-2}$ at least scales as $\Delta_{\vec{k}}^{-2} \propto (k_\alpha - \bar{k}_\alpha)^{-2}$ in the vicinity of a manifold $\bar{k}$ where $\Delta_{\vec{k}} = 0$ (if $\Delta_{\vec{k}} = 0$ occurs at the boundary of the integration volume the divergence is even more severe). We thus conclude that nonexponential decay or a divergent correlation length can only appear for $\delta = 0$ and $(2n_\sigma - 1) = 0$. Both conditions can only hold for $\gamma_a = 0$, i.e., if the photon decay vanishes.

B. Correlations in one dimension

We now examine correlations in a one-dimensional (1D) chain, $\mathcal{C}(x)$ with $-N/2 \leqslant x \leqslant N/2$, Eq. (6), considering N to be a multiple of 4, so that the Bloch modes are distributed symmetrically around the cavity frequency. We first focus on $N = 12$ with $J = 0.5g$ or $10g$, for which we show n_a as a function of the pump in Fig. 2(a). Both cases undergo very similar and characteristic transitions into and out of lasing [cf. Fig. 1(i)]. We select two pumping rates representative of the lasing (1) and thermal (2) regimes and plot $\mathcal{C}(x)$ as a function of the detuning $\Delta = \omega_\sigma - \omega_a$ and the separation x between the cavities in Fig. 2(b). For $|\Delta| < 2J$, $\mathcal{C}(x)$ oscillates as $\cos(\bar{k}x)$, where $\bar{k}$ and $-\bar{k}$ are the (degenerate) modes closest to resonance with the emitters, i.e., $|\Delta| \approx 2J\cos\bar{k}$. The correlation length is longer in the lasing regime (1), increases for larger J, and becomes maximal for $|\Delta| = 2J$ in each case, i.e., when the emitters are in resonance with the edges of the Bloch band. For $J = 10g$ it becomes larger than the finite-size array of $N = 12$ considered here since the frequency separation between Bloch modes is so large that the emitters only populate one mode efficiently. Note that any decay of correlations is entirely due to destructive interference between different Bloch-mode contributions.

Let us now explore $|\Delta| \leqslant 2J$, where the emitters are on resonance with the Bloch band and photonic modes are appreciably populated. For a long chain, $N \gg 1$, and large tunneling rates, $J \gg g$, analytical estimates can be found for the correlations $\mathcal{C}(x)$ (see Appendix C). In agreement with Fig. 2, these show exponential decay modulated by an oscillation. We thus fit a function $f(x) = [c_1\cos(\nu x) + c_2\sin(\nu x)]\exp(-\lambda x)$ to $\mathcal{C}(x)$ in the entire range of tunneling rates J and extract the inverse correlation length λ from the fit (see Appendix C for examples). Figure 2(c) shows λ for three cases: $\Delta = 0$ (solid), $\Delta = J$ (dotted), and $\Delta = 2J$ (dashed) for a chain of $N = 108$ cavities, which has Bloch modes in resonance with the emitters for all considered values of Δ so that finite-size effects are suppressed. As a second main result of our work we observe a clear transition from the regime with $J < g$, where $\lambda \propto -\ln J$, to the regime $J > g$, where $\lambda \propto J^{-1}$ for $J \gg |\Delta|$ and $\lambda \propto J^{-1/2}$ for $2J = |\Delta|$. These behaviors are also found from analytical estimates for $N \to \infty$ (the details of the derivations are provided in Appendix C).

V. LOCAL PROPERTIES IN 1D CHAINS

Finally, we present some experimentally observable and distinctive local signatures of the collective lasing regime in the array, as a function of Δ. In Figs. 3(a)–3(i) we plot n_a and n_σ, computed from Eqs. (4), for various arrays. Each underlying Bloch mode n_k enters its own lasing regime at $\omega_\sigma = \omega_k$. This results in the enhancement of n_a to a fixed value, given by the resonant one-emitter case n_a^{L}, while the emitter population decreases to $n_\sigma^{\mathrm{L}} \approx 1/2$ from its saturation value of 1 [46]. Note that these traits are independent of g, N, and J once the system is strongly enough coupled to reach the lasing regime [47]. With these conditions we compare various arrays, i.e., $N = 4$, 12, 32 and $J/g = 0.5$, 10, 50, and the one-emitter laser (showing n_a only for that case); see Fig. 3. Interactions as small as $J \lesssim 0.5g$ (Fig. 3, upper row) are not enough to make a qualitative difference from the $N = 1$ case in the local populations [48]. The width in detuning of the apparent single broad resonance is given by $2\Delta_{\max} = \sqrt{P_\sigma(\kappa_\sigma - P_\sigma)}$ [49]. Increasing interactions, $J > g$ (other rows), splits the Bloch modes apart so that they can be selectively addressed by changing detuning. The excitation is distributed equally among the driven modes so, at resonance, $n_{k=0,\pi} = N n_a^{\mathrm{L}}$ and $n_{\pm k} = N n_a^{\mathrm{L}}/2$ for the other central modes. This results in a series of peaks for n_a of equal height n_a^{L} and width $2\Delta_{\max}$. When the width is smaller than the average separation between Bloch modes, approximately given by $4J/N$ (or $4J/(N-1)$ for odd N), a plateau forms in the populations that extends for $|\Delta| \leqslant 2J$; cf. Fig. 3(f). At this point, increasing N does not affect the results qualitatively.

Another very distinctive feature of the collective lasing is provided by the emitter photoluminescence spectrum $S(\Gamma_d,\omega)$, where Γ_d is the detector linewidth. In order to compute it, we make the semiclassical approximation of substituting the cav-

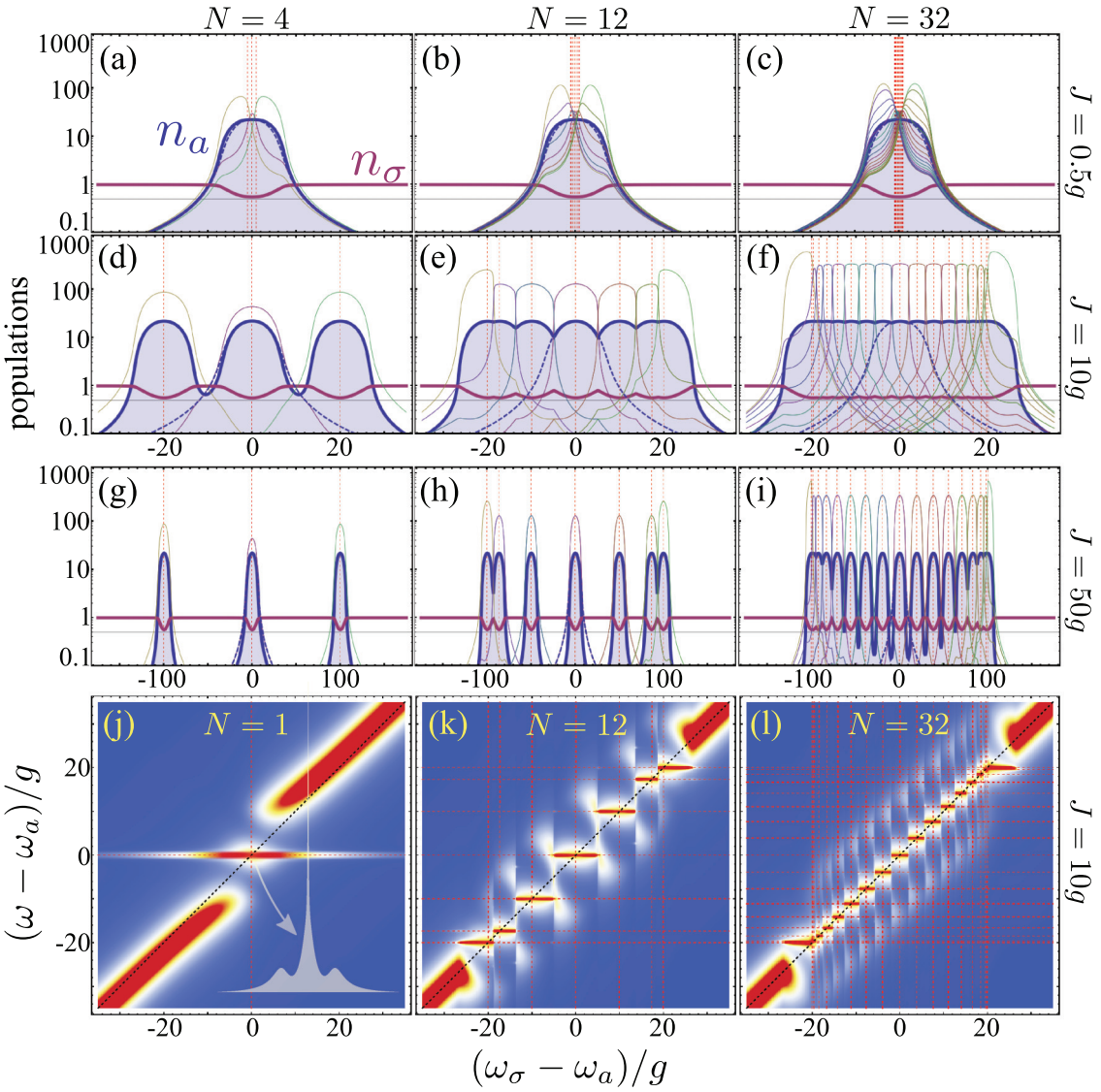

FIG. 3. (Color online) (a)–(i) Populations of the different modes involved, when sweeping the emitter frequency ω_σ through the system resonances (vertical red dashed lines): n_a in solid and filled blue, n_σ in solid pink, the Bloch modes n_k with thin lines and n_a for the case $N = 1$ in dashed blue as a reference. (j) Emitter spectrum of emission for $N = 1$ and varying ω_σ, showing a Mollow triplet around resonance. In inset, the line shape at resonance. In (k) and (l), the spectra for cases (e) and (f), respectively. We use a temperature color code which goes from blue (0) to red (maximum values). Parameters are $N = 4$, 12, 32 and $J = 0.5g$, $10g$, $50g$, varying as indicated. Also, $P_\sigma = 5g$, $\gamma_a = 0.1g$, $\gamma_\sigma = 0.01g$, $\Gamma_d = 0.3g$.

ity fields by a multimode laser that acts independently on each of the emitters. That is, we consider the approximated Hamiltonian $H_{\rm ML} = \sum_{\vec r}[\omega_\sigma \sigma_{\vec r}^\dagger \sigma_{\vec r} + \Omega(t)\sigma_{\vec r}^\dagger + \Omega^*(t)\sigma_{\vec r}]$, where $\Omega(t) = \sum_{\vec k} g\sqrt{n_{\vec k}/N} e^{-i\omega_{\vec k} t}$ is the time-dependent multimode field. Additionally, the emitters are still being excited by the incoherent pump and decaying, through the usual Lindblad forms. There is no steady state for this approximated model (for $N > 1$) but a quasisteady state, that is, an ever oscillating solution for the density matrix elements around a mean point. Such mean point is given (approximately) by the exact solution of the full master equation or the rate equations, which do have a steady state. That is, $\sum_{\vec k} G_{\vec k,\vec r}\langle p_{\vec k}\sigma_{\vec r}^\dagger\rangle e^{-i\omega_{\vec k} t}$ is well estimated by $\Omega(t)\langle\sigma_{\vec r}^\dagger\rangle_{\rm ML}$, where $\langle\cdot\rangle_{\rm ML}$ is the mean value obtained with the approximated master equation and Hamiltonian $H_{\rm ML}$ for the emitters only. The fact that the first term is $\vec r$ independent compels $\Omega(t)$ to be $\vec r$ independent as well. We describe the resulting time-dependent dynamics in the following way: First, we solve the new master equation with $H_{\rm ML}$, and obtain its time-dependent spectrum of emission [50,51], $S_{\rm ML}(\Gamma_d,\omega,t)$, by coupling the emitter very weakly to another two-level system, which radiatively decays at a rate Γ_d, and plays the role of the detector. The population of this detector is exactly the time-dependent spectrum of our emitter [52]. Then, we take its average over time, once the quasisteady state is reached, starting at a point in time which we call t_0: $S(\Gamma_d,\omega) \approx \int_{t_0}^{t_0+T} S_{\rm ML}(\Gamma_d,\omega,t)dt/T$. This is a very good approximation in the case $N = 1$ [17,30] for which there is a simple analytical formula [53].

Despite the incoherent pump, a Mollow triplet forms [17,30,53,54] whenever $\omega_\sigma = \omega_k$ for some k, thanks

to the effective multi-Bloch-mode coherent drive $\Omega(t)$. In Figs. 3(j)–3(l), we compare $N = 1$, 12, and 32, for varying Δ. The Rayleigh peak, produced by the elastically scattered cavity laser field, is pinned at the cavity frequency for a single mode excitation (j), with small linewidth given by the detector only Γ_d (as in this approximation the cavity has an infinitely long lifetime). In the multimode case, Figs. 3(k) and 3(l), the Rayleigh peak jumps from Bloch mode to Bloch mode, depending on which one dominates, in correspondence with the population plateaus of Figs. 3(e) and 3(f). The sidebands are positioned at $\omega_k \pm 2\sqrt{2}g\sqrt{n_a^{\mathrm{L}}}$, around resonance with a degenerate Bloch mode ω_k, and at $\omega_k \pm 2g\sqrt{n_a^{\mathrm{L}}}$, with the edge modes. Therefore, high N and closely packed Bloch modes give rise to two Mollow continuous sidebands at $\omega_\sigma \pm 2\sqrt{2}g\sqrt{n_a^{\mathrm{L}}}$, extending over $|\Delta| \leqslant 2J$.

ACKNOWLEDGMENTS

J.R.-R. acknowledges the hospitality of Technical University Munich, where part of this work was done. E.d.V. acknowledges support from the Alexander von Humboldt-Foundation, the Spanish MINECO under Contract No. MAT2011-22997 and the IEF project SQUIRREL (623708), P.G. from Research Grant No. PNII-ID-PCE-2011-3-0091, and M.J.H. from Emmy Noether Grant No. HA 5593/1-1 and CRC 631 (both DFG).

APPENDIX A: EQUATIONS OF MOTION FOR THE CORRELATORS

In this section, we derive the system equations of motion in the case of a one-dimensional array. They can be trivially extended to higher dimensions.

The most general operator in the system reads $\langle O\rangle = \langle \Pi_k p_k^{\dagger m_k} p_k^{n_k} \Pi_j \sigma_j^{\dagger \mu_j} \sigma_j^{\nu_j}\rangle$. From the master equation in the main text, we obtain the equations of motion for the set of relevant operators by means of the general relation $\partial_t\langle O\rangle = \mathrm{Tr}(O\partial_t\rho)$ as

$$\partial_t\left\langle \Pi_k p_k^{\dagger m_k} p_k^{n_k} \Pi_j \sigma_j^{\dagger\mu_j}\sigma_j^{\nu_j}\right\rangle = \sum_{\bar m_1,\bar n_1,\dots\bar\mu_1,\bar\nu_1\dots} R^{m_1,n_1,\dots\mu_1,\nu_1\dots}_{\bar m_1,\bar n_1,\dots\bar\mu_1,\bar\nu_1\dots} \times \left\langle \Pi_k p_k^{\dagger \bar m_k} p_k^{\bar n_k} \Pi_j \sigma_j^{\dagger\bar\mu_j}\sigma_j^{\bar\nu_j}\right\rangle. \tag{A1}$$

The diagonal elements in R, involving all modes and emitters, are given by [55]

$$\begin{aligned} R^{m_1,n_1,\dots\mu_1,\nu_1\dots}_{m_1,n_1,\dots\mu_1,\nu_1\dots} &= \sum_k\left[i\omega_k(m_k-n_k) - \frac{\gamma_a}{2}(m_k+n_k)\right] \\ &+ \sum_j\left[i\omega_\sigma(\mu_j-\nu_j) - \frac{\gamma_\sigma+P_\sigma}{2}(\mu_j+\nu_j) - \frac{\gamma_\phi}{2}(\mu_j-\nu_j)^2\right]. \end{aligned} \tag{A2}$$

We have included in these elements the effect of pure dephasing at a rate γ_ϕ, added to the master equations through the Lindblad term $\gamma_\phi\mathcal{L}_{\sigma_j^\dagger\sigma_j}(\rho)$. This only results in the increase of the total decoherence rate into $\Gamma = \gamma_a + P_\sigma + \gamma_\sigma + \gamma_\phi$ [56]. Next, the incoherent pumping of emitter j affects only elements concerning such emitter so that for all j,

$$R^{\dots\mu_j,\nu_j\dots}_{\dots\mu_j,\nu_j\dots} = P_\sigma\mu_j\nu_j. \tag{A3}$$

Finally, the coupling between mode k and emitter j, provides the elements:

$$R^{m_k,n_k,\mu_j,\nu_j}_{m_k-1,n_k,1-\mu_j,\nu_j} = iG_{kj}m_k(1-\mu_j), \tag{A4a}$$

$$R^{m_k,n_k,\mu_j,\nu_j}_{m_k,n_k-1,\mu_j,1-\nu_j} = -iG^*_{kj}n_k(1-\nu_j), \tag{A4b}$$

$$R^{m_k,n_k,\mu_j,\nu_j}_{m_k+1,n_k,1-\mu_j,\nu_j} = iG^*_{kj}\mu_j, \tag{A4c}$$

$$R^{m_k,n_k,\mu_j,\nu_j}_{m_k,n_k+1,\mu_j,1-\nu_j} = -iG_{kj}\nu_j \tag{A4d}$$

$$R^{m_k,n_k,\mu_j,\nu_j}_{m_k+1,n_k,\mu_j,1-\nu_j} = -2iG^*_{kj}\mu_j(1-\nu_j), \tag{A4e}$$

$$R^{m_k,n_k,\mu_j,\nu_j}_{m_k,n_k+1,1-\mu_j,\nu_j} = 2iG_{kj}\nu_j(1-\mu_j), \tag{A4f}$$

and zero everywhere else.

With these general rules, we can write the equations for the main correlators of interest, starting with the populations of the modes, $n_k = \langle p_k^\dagger p_k\rangle$ and emitters $n_j = \langle\sigma_j^\dagger\sigma_j\rangle$:

$$\partial_t n_j = -(P_\sigma+\gamma_\sigma)n_j + P_\sigma - 2\sum_k \mathrm{Im}[G^*_{kj}\langle p_k^\dagger\sigma_j\rangle], \tag{A5a}$$

$$\partial_t n_k = -\gamma_a n_k + 2\sum_j \mathrm{Im}[G^*_{kj}\langle p_k^\dagger\sigma_j\rangle], \tag{A5b}$$

$$\begin{aligned} \partial_t\langle p_k^\dagger\sigma_j\rangle &= -\left[\frac{\Gamma}{2} + i(\omega_\sigma-\omega_k)\right]\langle p_k^\dagger\sigma_j\rangle \\ &+ iG_{kj}[n_j - n_k + 2\langle p_k^\dagger p_k\sigma_j^\dagger\sigma_j\rangle] \\ &+ \sum_{l\neq j} iG_{kl}\langle\sigma_l^\dagger\sigma_j\rangle + \sum_{q\neq k}(-iG_{ql})\langle p_k^\dagger p_q\rangle \\ &+ \sum_{q\neq k} 2iG_{qj}\langle p_k^\dagger p_q\sigma_j^\dagger\sigma_j\rangle. \end{aligned} \tag{A5c}$$

The equations for the correlators that represent the indirect coupling between different emitters or Bloch modes are

$$\begin{aligned} \partial_t\langle\sigma_l^\dagger\sigma_j\rangle &= -(P_\sigma+\gamma_\sigma)\langle\sigma_l^\dagger\sigma_j\rangle \\ &+ \sum_k i[G^*_{kl}\langle p_k^\dagger\sigma_j\rangle - G_{kj}\langle p_k\sigma_l^\dagger\rangle] \\ &+ \sum_k 2i[G_{kj}\langle p_k\sigma_l^\dagger\sigma_j^\dagger\sigma_j\rangle - G^*_{kl}\langle p_k^\dagger\sigma_l^\dagger\sigma_l\sigma_j\rangle], \end{aligned} \tag{A6a}$$

$$\begin{aligned} \partial_t\langle p_k^\dagger p_q\rangle &= -[\gamma_a - i(\omega_k-\omega_q)]\langle p_k^\dagger p_q\rangle \\ &+ \sum_j i[G_{kj}\langle p_q\sigma_j^\dagger\rangle - G^*_{qj}\langle p_k^\dagger\sigma_j\rangle]. \end{aligned} \tag{A6b}$$

Within the formal scheme of the cluster-expansion method, Eq. (A6a) is of the same order as the Bloch-mode populations n_k. This is owed to the dominant Jaynes-Cummings interaction in the system, which can be used to establish a formal equivalence between an electronic transition and photon creation or absorption [41]. In the thermal and lasing regimes investigated in the main text, the influence of these correlations is small and, therefore, neglected in order to keep the formal solution of the equations as simple as possible.

Finally, the intensity-intensity correlations are given by

$$\begin{aligned}\partial_t\langle p_k^\dagger p_k\sigma_l^\dagger\sigma_l\rangle = &-(\gamma_a+P_\sigma+\gamma_\sigma)\langle p_k^\dagger p_k\sigma_l^\dagger\sigma_l\rangle + P_\sigma n_k\\ &+i(G_{kl}^*\langle p_k^\dagger p_k^\dagger p_k\sigma_l\rangle - G_{kl}\langle p_k^\dagger p_k p_k\sigma_l^\dagger\rangle)\\ &+i\sum_{q\neq k}(G_{ql}^*\langle p_q^\dagger p_k^\dagger p_k\sigma_l\rangle - G_{ql}\langle p_q^\dagger p_k p_k\sigma_l^\dagger\rangle)\\ &+i\sum_{j\neq l}(G_{kj}\langle p_k\sigma_l^\dagger\sigma_l\sigma_j^\dagger\rangle - G_{kj}^*\langle p_k^\dagger\sigma_j\sigma_l^\dagger\sigma_l\rangle).\end{aligned} \tag{A7}$$

Analytical solution of the rate equations for $N = 1$

In the case $N = 1$, we have only a single emitter and photonic mode so $F_k \to F$ and the rate equations in the steady state reduce to

$$0 = -\gamma_a n_a + F n_a(2n_\sigma - 1) + F n_\sigma, \tag{A8a}$$

$$0 = -(P_\sigma + \gamma_\sigma + F)n_\sigma + P_\sigma - (2n_\sigma - 1)F n_a. \tag{A8b}$$

The solution of these equations reads

$$n_a = \frac{F(2P_\sigma - \zeta_\sigma - \gamma_a) - \gamma_a\zeta_\sigma + \chi^2}{4F\gamma_a}, \tag{A9}$$

$$n_\sigma = \frac{P_\sigma - \gamma_a n_a}{\zeta_\sigma} \tag{A10}$$

with $\chi^2 = \sqrt{[F(2P_\sigma + \zeta_\sigma + \gamma_a) + \gamma_a\zeta_\sigma]^2 - 8FP_\sigma\zeta_\sigma(F + \gamma_a)}$ and $\zeta_\sigma = P_\sigma + \gamma_\sigma$.

APPENDIX B: FAST DECAY OF CORRELATIONS IN THE LIMIT OF LOW PUMPING

Our approach is expected to yield accurate results in the lasing and thermal regimes, where $P_\sigma > \gamma_\sigma, \gamma_a$ and the emitters are population inverted, $n_\sigma > 1/2$. As it shows the largest correlation length, we focus on the lasing regime in the main text. Yet in the low pumping regimes, complementary to the regimes where our considerations apply, one expects correlations to decay faster than in the lasing regime.

In the limit of vanishing pumping, where the emitter occupancies are very low, $n_\sigma \ll 1$, one can approximate the emitters by harmonic oscillators and our model maps to a set of coupled harmonic oscillators. In this exactly solvable, linear regime, the width of the Lorentzian distribution in Eq. (5) is larger than in the lasing regime and therefore correlations $\mathcal{C}(\vec{r})$ decay faster.

Moreover, increasing the pumping to transfer some non-negligible population to the cavities, $n_a \sim 1$, the array enters the quantum regime. The nonlinearity of the emitters acts as a repulsive on-site interaction between excitations in the cavity array. Similar to the equilibrium situation, this interaction will keep excitations from delocalizing across the array and correlations will remain short ranged [57]. It is important to note here that the nonlinearity of a Jaynes-Cummings system scales as the square root of the photon number in the cavity, $\sqrt{n_a}$. The coupling between cavities, in turn, is quadratic in the photon operators $(Ja_j a_{j+1}^\dagger + \text{H.c.})$ so that its strength scales linearly with n_a. Hence for higher input powers and thus higher photon numbers n_a, the influence of the nonlinearity is weakened. As one enters the lasing regime, where our approach applies, one thus finds longer range correlations.

APPENDIX C: ESTIMATES FOR FIELD CORRELATIONS IN ONE DIMENSION IN THE LIMIT $N \to \infty$

For one dimension, $m = 1$, the momentum distribution in the stationary state reads $n_k = \frac{\kappa_\sigma\Gamma}{4}\frac{n_\sigma}{(\delta/2)^2+\Delta_k^2}$, which is a Lorentzian in the detunings $\Delta_k = \Delta - 2J\cos k$, and for $N \to \infty$ the field correlations read

$$\mathcal{C}(x) = \frac{1}{n_a 2\pi}\int_{-\pi}^{\pi} dk e^{-ixk} n_k. \tag{C1}$$

With n_k a real and even function of k, it is obvious that $\mathcal{C}(x)$ is also real and even as a function of the distance x. Therefore in what follows we consider only the case $x \geqslant 0$. Up to the prefactor $\frac{\kappa_\sigma\Gamma n_\sigma}{4n_a J^2}$, and bearing in mind that x takes only integer values, the correlations are obtained by calculating a Fourier transform of the form

$$C_n = \frac{1}{2\pi}\int_{-\pi}^{\pi}\frac{e^{ikn}}{(2\cos k - \widetilde{\Delta})^2 + \widetilde{\delta}^2}\,dk, \quad n = 0,1\ldots \tag{C2}$$

with the parameters $\widetilde{\Delta}$ and $\widetilde{\delta}$ easy to identify as $\widetilde{\Delta} = \Delta/J$ and $\widetilde{\delta} = \delta/(2J)$. One rearranges the expression under the integral as

$$\frac{1}{(2\cos k - \widetilde{\Delta})^2 + \widetilde{\delta}^2} = \frac{1}{2i\widetilde{\delta}}\frac{1}{2\cos k - \widetilde{\Delta} - i\widetilde{\delta}} + \text{c.c.}, \tag{C3}$$

so that one has to compute

$$C_n = \frac{1}{4\pi i\widetilde{\delta}}\int_{-\pi}^{\pi}\frac{e^{ikn}}{2\cos k - u}\,dk + \text{c.c.}, \tag{C4}$$

where u denotes the complex quantity $u = \widetilde{\Delta} + i\widetilde{\delta} = J^{-1}(\Delta + i\delta/2)$. This integral is solved by introducing the new variable $z = e^{ik}$, which runs on the unit circle $\mathcal{C}_1$,

$$C_n = \frac{-1}{4\pi\delta}\int_{\mathcal{C}_1}\frac{z^n}{z^2 - u\,z + 1}\,dz + \text{c.c.} \tag{C5}$$

The poles of the integrand are the roots of the denominator $\zeta_{1,2}$, and satisfy $\zeta_1 + \zeta_2 = u$ and $\zeta_1\,\zeta_2 = 1$. There are two possibilities, either (i) $|\zeta_1| < 1 < |\zeta_2|$, or (ii) $|\zeta_1| = 1 = |\zeta_2|$. Representing the roots as $\zeta_2 = e^\lambda e^{iq}$ and $\zeta_1 = e^{-\lambda}e^{-iq}$, case (i) amounts to $\lambda > 0$ and ζ_1 lying inside the unit circle. The

residue theorem then gives

$$C_n = \frac{i}{2\widetilde{\delta}} \frac{1}{\zeta_2 - \zeta_1} \zeta_1^n + \text{c.c.} \tag{C6}$$

This shows that the correlations oscillate along the chain with a wave number q and decay exponentially with the inverse decay length λ.

Case (ii) corresponds to $\lambda = 0$, when both roots are found on $\mathcal{C}_1$. This takes place when $u = \zeta_1 + \zeta_2 = 2\cos q$, i.e., u is real and belongs to the interval $[-2,2]$. With poles on the integration path the integral is divergent. Still, it makes sense to consider this as a limit case, with u approaching the segment $[-2,2]$ of the real axis. Then ζ_1 approaches the unit circle from within, and the correlation length $1/\lambda$ goes to infinity. The system becomes critical. The requirements on the system parameters for achieving criticality are $\delta \to 0$ and $|\Delta| \leqslant 2J$. It also follows that q is the momentum of the resonant Bloch mode.

It is straightforward to relate the quantities λ and q, to the system parameters but the expressions are cumbersome. Some qualitative features are easily obtained though, and they describe different regimes of correlation behavior.

A first situation is encountered when u lies in the complex plane far away from the critical interval $[-2,2]$. For $\widetilde{\Delta}$ and $\widetilde{\delta}$ large, this corresponds to small J values, since $\widetilde{\Delta} \propto J^{-1}$ and $\widetilde{\delta} \propto J^{-1}$. In this case λ is large and in the relation $\zeta_1 + \zeta_2 = u$ the small root ζ_1 becomes negligible. It follows that $\lambda = \ln|\zeta_2| \simeq \ln|u| \propto -\ln J$.

A completely different behavior is seen when u is close to the segment $[-2,2]$. In this regime J is large to make $\widetilde{\delta}$ small. Also, Δ, J are of the same magnitude and obey $|\Delta| \leqslant 2J$, to keep $\widetilde{\Delta}$ within the limit of the interval. In this case $\lambda \simeq 0$, both roots are close to the unit circle. Therefore both contribute to the sum, and one can write

$$\tfrac{1}{2}u = \tfrac{1}{2}(\widetilde{\Delta} + i\widetilde{\delta}) = \cosh\lambda\cos q + i\sinh\lambda\sin q. \tag{C7}$$

With λ small, one has $\cosh\lambda \simeq 1$ and $\sinh\lambda \simeq \lambda$ and by identifying the real and imaginary parts, it follows that $\cos q = \widetilde{\Delta}/2 = \Delta/(2J)$ and

$$\lambda = \frac{\widetilde{\delta}}{2\sin q} = \frac{\delta/2}{\sqrt{4J^2 - \Delta^2}} = \sqrt{\frac{g^2\Gamma}{\gamma_a(4J^2 - \Delta^2)}\left[\frac{\gamma_a\Gamma}{4g^2} - (2n_\sigma - 1)\right]}. \tag{C8}$$

With Δ of the same order as J, one obtains $\lambda \propto J^{-1}$.

The above result holds for $\widetilde{\Delta}$ not too close to the endpoints of the critical interval, where $\sin q$ becomes small and division by it gives rise to large values of λ. This is seen in the final expression for λ, in which Δ approaching $2J$ leads to a singularity. Therefore this case requires a separate, more careful consideration, since now q becomes a small quantity, too. Expanding up to the second order in terms of the small arguments, Eq. (C7) becomes

$$\tfrac{1}{2}(\widetilde{\Delta} + i\widetilde{\delta}) \simeq 1 + \tfrac{1}{2}\lambda^2 - \tfrac{1}{2}q^2 + i\lambda q. \tag{C9}$$

To keep the discussion simple we discuss the case $\Delta = 2J$, or $\widetilde{\Delta} = 2$. Actually this illustrates the more general situation in which $1 - \widetilde{\Delta}/2$ is a small quantity of a higher than second order. Then, from Eq. (C9) we find $\lambda = q$ and $\lambda^2 = \widetilde{\delta}/2 = \delta/(4J)$. More precisely

$$\lambda = \left\{\frac{g^2\Gamma}{4\gamma_a J^2}\left[\frac{\gamma_a\Gamma}{4g^2} - (2n_\sigma - 1)\right]\right\}^{1/4}. \tag{C10}$$

Note that now $\lambda \propto J^{-1/2}$.

Examples for the fits

In this section we provide some examples for the fits of functions $f(x) = [c_1\cos(\nu x) + c_2\sin(\nu x)]\exp(-\lambda x)$ to the normalized correlations $\mathcal{C}(x)$. These examples are shown in Fig. 4 and illustrate the excellent quality of the fits. Only for $J \ll g$ the fitting procedure is more fragile as correlations decay very fast and are thus indistinguishable from zero for most values of x.

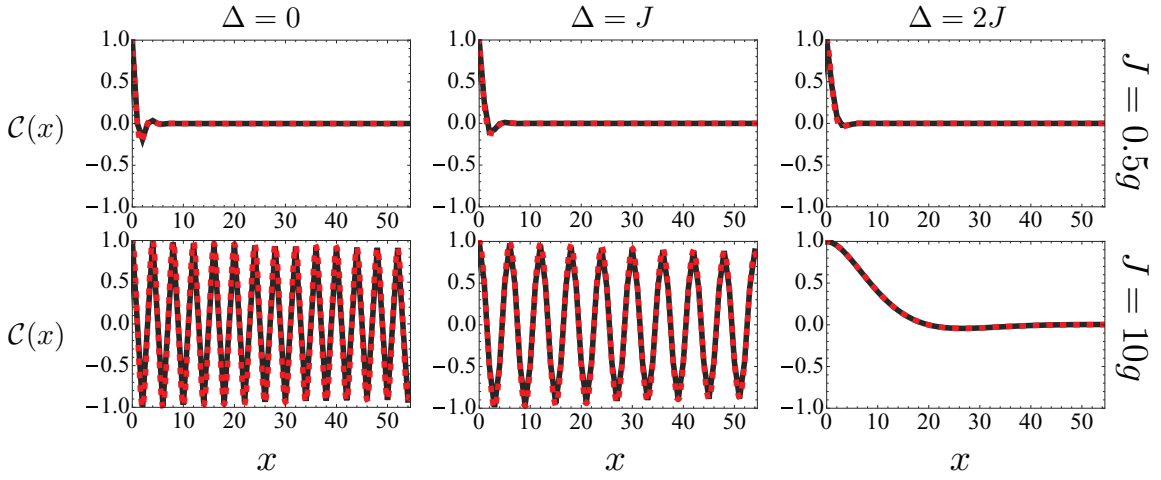

FIG. 4. (Color online) Examples for fits of functions $f(x) = [c_1\cos(\nu x) + c_2\sin(\nu x)]\exp(-\lambda x)$ to the normalized correlations $\mathcal{C}(x)$ for $N = 108$ and the parameters Δ and J given in the labels of the columns and rows. Other parameters are $\gamma_a = 0.1g$, $\gamma_\sigma = 0.01g$, $P_\sigma = 5g$.

[1] M. J. Hartmann, F. G. S. L. Brandão, and M. B. Plenio, Nat. Phys. **2**, 849 (2006).
[2] A. D. Greentree, C. Tahan, J. H. Cole, and L. C. L. Hollenberg, Nat. Phys. **2**, 856 (2006).
[3] D. G. Angelakis, M. F. Santos, and S. Bose, Phys. Rev. A **76**, 031805 (2007).
[4] M. Hartmann, F. Brandão, and M. Plenio, Laser Photon. Rev. **2**, 527 (2008).
[5] A. Tomadin and R. Fazio, J. Opt. Soc. Am. B **27**, A130 (2010).
[6] A. A. Houck, H. E. Tureci, and J. Koch, Nat. Phys. **8**, 292 (2012).
[7] I. Carusotto and C. Ciuti, Rev. Mod. Phys. **85**, 299 (2013).
[8] I. Carusotto, D. Gerace, H. E. Tureci, S. De Liberato, C. Ciuti, and A. Imamoğlu, Phys. Rev. Lett. **103**, 033601 (2009).
[9] M. J. Hartmann, Phys. Rev. Lett. **104**, 113601 (2010).
[10] F. Nissen, S. Schmidt, M. Biondi, G. Blatter, H. E. Türeci, and J. Keeling, Phys. Rev. Lett. **108**, 233603 (2012).
[11] R. O. Umucalılar and I. Carusotto, Phys. Rev. Lett. **108**, 206809 (2012).
[12] C.-E. Bardyn and A. İmamoğlu, Phys. Rev. Lett. **109**, 253606 (2012).
[13] Y. Mu and C. M. Savage, Phys. Rev. A **46**, 5944 (1992).
[14] J. McKeever, A. Boca, A. D. Boozer, J. R. Buck, and H. J. Kimble, Nature (London) **425**, 268 (2003).
[15] O. Astafiev, K. Inomata, A. O. Niskanen, T. Yamamoto, Y. A. Pashkin, Y. Nakamura, and J. S. Tsai, Nature (London) **449**, 588 (2007).
[16] M. Nomura, N. Kumagai, S. Iwamoto, Y. Ota, and Y. Arakawa, Nat. Phys. **6**, 279 (2010).
[17] E. del Valle and F. P. Laussy, Phys. Rev. A **84**, 043816 (2011).
[18] P. Gartner, Phys. Rev. A **84**, 053804 (2011).
[19] G. Yeoman and G. M. Meyer, Phys. Rev. A **58**, 2518 (1998).
[20] F. P. Laussy, A. Laucht, E. del Valle, J. J. Finley, and J. M. Villas-Bôas, Phys. Rev. B **84**, 195313 (2011).
[21] A. Auffèves, D. Gerace, S. Portolan, A. Drezet, and M. F. Santos, New J. Phys. **13**, 093020 (2011).
[22] A. N. Poddubny, M. M. Glazov, and N. S. Averkiev, Phys. Rev. B **82**, 205330 (2010).
[23] C. Gies, M. Florian, P. Gartner, and F. Jahnke, Opt. Express **19**, 14370 (2011).
[24] I. Bloch, J. Dalibard, and W. Zwerger, Rev. Mod. Phys. **80**, 885 (2008).
[25] S. Diehl, A. Micheli, A. Kantian, B. Kraus, H. P. Bucheler, and P. Zoller, Nat. Phys. **4**, 878 (2008).
[26] P. Schindler, M. Müller, D. Nigg, J. T. Barreiro, E. A. Martinez, M. Hennrich, T. Monz, S. Diehl, P. Zoller, and R. Blatt, Nat. Phys. **9**, 361 (2013).
[27] D. Marcos, A. Tomadin, S. Diehl, and P. Rabl, New J. Phys. **14**, 055005 (2012).
[28] E. Altman, L. M. Sieberer, L. Chen, S. Diehl, and J. Toner, arXiv:1311.0876.
[29] L. M. Sieberer, S. D. Huber, E. Altman, and S. Diehl, Phys. Rev. Lett. **110**, 195301 (2013).
[30] E. del Valle and F. P. Laussy, Phys. Rev. Lett. **105**, 233601 (2010).
[31] J. Raftery, D. Sadri, S. Schmidt, H. E. Türeci, and A. A. Houck, arXiv:1312.2963 [Phys. Rev. X (to be published)].
[32] A. Majumdar, A. Rundquist, M. Bajcsy, V. D. Dasika, S. R. Bank, and J. Vuckovic, Phys. Rev. B **86**, 195312 (2012).
[33] A. Rundquist, A. Majumdar, M. Bajcsy, V. D. Dasika, S. Bank, and J. Vuckovic, in *CLEO: 2013* (Optical Society of America, San Jose, California, 2013), p. CM4F.7.
[34] M. Abbarchi, A. Amo, V. G. Sala, D. D. Solnyshkov, H. Flayac, L. Ferrier, I. Sagnes, E. Galopin, A. Lemaître, G. Malpuech, and J. Bloch, Nat. Phys. **9**, 275 (2013).
[35] G. Lepert, M. Trupke, M. J. Hartmann, M. B. Plenio, and E. A. Hinds, New J. Phys. **13**, 113002 (2011).
[36] E. del Valle, F. P. Laussy, and C. Tejedor, Phys. Rev. B **79**, 235326 (2009).
[37] D. Braun, Phys. Rev. Lett. **89**, 277901 (2002).
[38] N. S. Averkiev, M. M. Glazov, and A. N. Poddubnyi, Sov. Phys. JETP **108**, 836 (2009).
[39] This is only below the maximum cavity population, reached at $P_\sigma \approx \kappa_\sigma/2$ [17]. We choose $\gamma_a = 0.1g$, $\gamma_\sigma = 0.01g$ and $P_\sigma = 5g$ as a paradigmatic example of the lasing regime for any N.
[40] K. Mølmer, Phys. Rev. A **55**, 3195 (1997).
[41] C. Gies, J. Wiersig, M. Lorke, and F. Jahnke, Phys. Rev. A **75**, 013803 (2007).
[42] A. Moelbjerg, P. Kaer, M. Lorke, B. Tromborg, and J. Mørk, IEEE J. Quantum Electron. **49**, 945 (2013).
[43] N. D. Mermin and H. Wagner, Phys. Rev. Lett. **17**, 1133 (1966).
[44] P. C. Hohenberg, Phys. Rev. **158**, 383 (1967).
[45] W. Rudin, *Real and Complex Analysis* (McGraw-Hill, New York, 1987).
[46] Also $g^{(2)} \approx 1$, although our rate equations do not provide this information .
[47] F. Laussy, E. del Valle, and J. Finley, Proc. SPIE **8255**, 82551G (2012).
[48] The rate equations provide for this case an analytical solution; cf. Eq. (10) in Appendix A.
[49] Estimation obtained by solving $n_a \approx n_a^{\mathrm{L}}\{1 - \frac{P_\sigma}{\kappa_\sigma}[1 + (\frac{2\Delta}{P_\sigma})^2]\} = 0$ in the detuned one-emitter laser [17].
[50] J. Eberly and K. Wódkiewicz, J. Opt. Soc. Am. **67**, 1252 (1977).
[51] J. H. Eberly, C. V. Kunasz, and K. Wódkiewicz, J. Phys. B: At. Mol. Phys. **13**, 217 (1980).
[52] E. del Valle, A. Gonzalez-Tudela, F. P. Laussy, C. Tejedor, and M. J. Hartmann, Phys. Rev. Lett. **109**, 183601 (2012).
[53] E. del Valle and F. P. Laussy, Wolfram Demonstrations Project (2013), http://demonstrations.wolfram.com/MollowTriplet/.
[54] B. R. Mollow, Phys. Rev. **188**, 1969 (1969).
[55] E. del Valle, *Microcavity Quantum Electrodynamics* (VDM Verlag, Saarbrücken, 2010).
[56] A. Gonzalez-Tudela, E. del Valle, E. Cancellieri, C. Tejedor, D. Sanvitto, and F. P. Laussy, Opt. Express **18**, 7002 (2010).
[57] M. P. A. Fisher, P. B. Weichman, G. Grinstein, and D. S. Fisher, Phys. Rev. B **40**, 546 (1989).